(Photo)Ionization of Tris(phenolato)iron(III) Complexes: Generation of Phenoxyl Radical as Ligand

J. Hockertz,[1] S. Steenken,*[,1] K. Wieghardt,*[,2] and P. Hildebrandt[1]

Contribution from the Max-Planck-Institut für Strahlenchemie, D-45413 Mülheim, Germany, Lehrstuhl für Anorganische Chemie I der Universität, D-44780 Bochum, Germany

Received April 5, 1993®

Abstract: FeL_p or FeL_o, the high-spin Fe(III) complexes of the hexadentate macrocyclic ligands 1,4,7-tris(3- or 5-*tert*-butyl-2-oxybenzyl)-1,4,7-triazacyclononane (L_o^{3-} or L_p^{3-}), which contain three o,o- or o,p-disubstituted phenolates, respectively, and which form a pseudo-octahedral environment (N_3O_3 donor set), have been photolyzed or chemically oxidized. The products were investigated employing (time resolved) UV/vis-detection and Mössbauer and resonance Raman (RR) spectroscopy. With light of ≈250 nm ($^1B_{1u} \leftarrow {}^1A_{1g}$ ($\pi-\pi^*$) transition of the ligand phenolates), in chlorinated hydrocarbon solvents, a monophotonic ionization takes place with quantum yields of 0.1 for FeL_o and ≈0.2 for FeL_p. In nonchlorinated solvents, FeL_p and FeL_o cannot be photoionized with ≈250-nm light. However, with 193-nm light ($^1E_{1u} \leftarrow {}^1A_{1g}$ ($\pi-\pi^*$) transition), ionization is possible also in CH_3CN, but in the absence of an electron scavenger, the solvated electrons recombine rapidly with the ionized complexes $FeL_{o/p}]^{\bullet+}$. By 254-nm photolysis of FeL_p in CH_2Cl_2, it is possible to produce solutions containing ≥90% in the oxidized form $FeL_p]^{\bullet+}$. This species can also be produced by reaction with $SO_4^{\bullet-}$ (rate constant 3.5×10^9 M^{-1} s^{-1} in 3:1 (v:v) CH_3CN/H_2O), $H_2PO_4^{\bullet}$, or $O_2^{\bullet+}$. In dry and inert solvents and in the solid state, $FeL_p]^{\bullet+}$ is stable at room temperature for months. Small quantities of water lead to a slow regeneration of FeL_p, accompanied by production of H^+. On the basis of Mössbauer data, supported by information from UV/vis and RR, in $FeL_p]^{\bullet+}$ the oxidation state of Fe(III) is retained; i.e., the missing electron (the hole) is located on (the phenolate part of) the ligand. RR investigations show that the electron deficiency is localized at an *individual* phenol moiety; i.e., it is present as a phenoxyl radical which remains coordinated to the high-spin Fe(III) core. FeL_o and FeL_p can be protonated in organic solvents. In the case of FeL_p, this leads to production of a dimer, $Fe_2(L_pH)_2]^{2+}$, in which the protons connect the monomers by forming two O···H···O hydrogen bridges between phenolates. The RR spectra of the protonated FeL_o and FeL_p complexes strongly resemble those of the oxidized species, indicating that protonation of a phenolate has an effect very similar to that of its one-electron oxidation and can in both cases be understood in terms of the resulting decrease in electron density at that site.

Introduction

In 1972, a stable organic radical was found as a constituent of the iron-containing nonheme metalloenzyme ribonucleotide reductase (RNR).[3] This enzyme catalyzes the conversion of ribonucleotides into 2′-deoxyribonucleotides. In its active form, RNR contains a tyrosyl radical and a mechanism for its action has been proposed.[4] A necessary condition[5] for the presence of tyrosyl is an antiferromagnetically[6] coupled Fe(III) dimer, Fe(III)$_2$. Both the tyrosyl radical and the nonheme Fe(III)$_2$ unit are localized in the subunit R2 of the enzyme. On the basis of X-ray studies on the inactive species metR2 (with Fe(III)$_2$, but a nonradical tyrosine group),[7] the OH function of the tyrosine group, which in the active form exists as the phenoxyl radical, is 5.3 Å apart from the adjacent iron atom[7-9]—a distance too large for a hyperfine interaction between the tyrosyl and the iron and for effective coordination.

In metR2, the environment of the tyrosine is hydrophobic.[7] In the active form of the enzyme, the situation seems to be similar, as concluded from ENDOR data which were interpreted in terms of a neutral tyrosyl radical not involved in a hydrogen bridge.[10] This view is supported by the resonance Raman (RR) spectra of the active form of R2 which show an undistorted C–O stretching band.[11,12] Also, the optical absorption spectra indicate that the tyrosyl is not involved in a hydrogen bond: On the basis of model studies on aroxyl radicals,[13] the *narrow* absorption band of active R2 near 410 nm[14,15] is indicative of a *non*-H-bonded tyrosyl.

Another example is photosystem II (photoinduced oxidation of water to molecular oxygen), in which two tyrosyl radicals are involved.[16-23] Tyrosyl radicals were also found in other proteins,[24] particularly in iron-containing enzymes.[25] In many cases, the structures of the active sites of these systems are not known, and

® Abstract published in *Advance ACS Abstracts*, October 15, 1993.

(1) Max-Planck-Institut.
(2) Universität Bochum.
(3) Ehrenberg, A.; Reichard, P. *J. Biol. Chem.* **1972**, *247*, 3485.
(4) Stubbe, J. A. *Annu. Rev. Biochem.* **1989**, *58*, 257.
(5) Fontecave, M.; Gerez, C.; Mansuy, D.; Reichard, P. *J. Biol. Chem.* **1990**, *265*, 10919.
(6) Peterson, L.; Gräslund, A.; Ehrenberg, A.; Sjöberg, B.-M.; Reichard, P. *J. Biol. Chem.* **1980**, *255*, 6706.
(7) Nordlund, P.; Sjöberg, B.-M.; Eklund, H. *Nature* **1990**, *345*, 593.
(8) Stubbe, J. A. *Chemtracts: Biochem. Mol. Biol.* **1990**, *1*, 444.
(9) Graden, J. A.; Valentine, J. S. *Chemtracts: Inorg. Chem.* **1991**, *3*, 97.
(10) Bender, C. J.; Sahlin, M.; Babcock, G. T.; Barry, B. A.; Chandrashekar, T. K.; Salowe, S. P.; Stubbe, J. A.; Lindström, B.; Peterson, L.; Ehrenberg, A.; Sjöberg, B.-M. *J. Am. Chem. Soc.* **1989**, *111*, 8076.
(11) Backes, G.; Sahlin, M.; Sjöberg, B.-M.; Loehr, T. M.; Sanders-Loehr, J. *Biochemistry* **1989**, *28*, 1923.
(12) Sjöberg, B.-M.; Sanders-Loehr, J.; Loehr, T. M. *Biochemistry* **1987**, *26*, 4242.
(13) Hockertz, J.; Steenken, S. Unpublished results.
(14) Mann, G. J.; Gräslund, A.; Ochiai, E.-I.; Ingemarson, R.; Thelander, L. *Biochemistry* **1991**, *30*, 1939.
(15) Lam, K.-Y.; Fortier, D. G.; Sykes, A. *J. Chem. Soc., Chem. Commun.* **1990**, 1019.
(16) Hanson, Ö.; Wydrzynski, T. *Photosynth. Res.* **1990**, *23*, 131.
(17) Svenson, B.; Vass, I.; Cedergren, E.; Styring, S. *EMBO J.* **1990**, *9*, 2051.
(18) Evelo, R. G.; Dikanov, S. A.; Hoff, A. J. *Chem. Phys. Lett.* **1989**, *159*, 25.
(19) Vass, I.; Styring, S. *Biochemistry* **1991**, *30*, 830.
(20) Babcock, G. T.; Barry, B. A.; Debus, R. J.; Hoganson, C. W.; Atamian, M.; McIntosh, L.; Sithole, I.; Yocum, C. F. *Biochemistry* **1989**, *28*, 9557.
(21) Vermaas, W. F. J.; Rutherford, A. W.; Hansson, Ö. *Proc. Natl. Acad. Sci. U.S.A.* **1988**, *85*, 8477.
(22) Hoganson, C. W.; Babcock, G. T. *Biochemistry* **1992**, *31*, 11874.
(23) Barry, B. A. *Photochem. Photobiol.* **1993**, *57*, 179.
(24) See ref 7.
(25) Retey, J. *Angew. Chem.* **1990**, *102*, 373.

0002-7863/93/1515-11222$04.00/0

the mechanisms of their reaction are not (fully) understood. For this reason, it appeared to be interesting to investigate simple model systems in which phenoxyl radicals are components of metal complexes and to determine their structures and reactivities.[26] Recently, the thermodynamically extremely stable tris(phenolato)iron(III) complexes FeL_o and FeL_p were synthesized[27] and structurally characterized[28] (see Chart I in Results and Discussion). We have now discovered that FeL_o and FeL_p can be photochemically or chemically oxidized by removal of a single electron from one of the phenolate ligands which leads to the formation of cationic Fe(III) complexes with *radical* nature, $FeL_o]^{\bullet+}$ and $FeL_p]^{\bullet+}$. These species may be considered model compounds for biocatalysts in which metal ions are associated with radicals such as tyrosyl. On the basis of UV/vis, resonance Raman, and Mössbauer data, these radicals have remarkable similarities in solution to the *protonated* parent compounds.

Experimental Section

The transition-metal complexes Fe^{III}[1,4,7-tris(3- or 5-*tert*-butyl-2-oxybenzyl)-1,4,7-triazacyclononane], abbreviated as FeL_o or FeL_p, and Ti^{IV}[1,4,7-tris(5-*tert*-butyl-2-oxybenzyl)-1,4,7-triazacyclononane]$^{+}$-PF_6^- ($TiL_p^+PF_6^-$) were synthesized as described.[27,28] The spectroscopic grade solvents CH_2Cl_2 (>99.5%, Merck), $ClCH_2CH_2Cl$ (99.8%, Merck), *n*-butyl chloride (≥99.5%, Fluka), and *sec*-butyl chloride (≥98%, Fluka) and CH_3CN (>99.8%, Merck) were used as received. 2-Methyltetrahydrofuran (2-MeTHF) was distilled to a purity of ≥99.8%. Argon (>99.998%) and other chemicals were of the highest purity available and were used without further purification. Water was purified with a Millipore Milli-Q system.

Photolysis with 254-nm Light. (a) For UV/vis spectroscopic studies, solutions of the parent compounds (optical densities (OD) at 254 nm ca. 2 cm^{-1}) in the chloroalkanes indicated, contained in 1 × 1 × 3 cm Suprasil quartz cells, were photolyzed at room temperature with the focused light of a medium-pressure mercury lamp (Phillips HPK 125W), while being stirred. The distance between the lamp and the cell was ca. 50 cm, sufficient for any light of 185 nm emitted by the lamp to be absorbed by the air. For the photochemically active wavelengths ($\lambda < 300$ nm), the spectral distribution of the emitted light at the position of the cell is dominated by the Hg* line at 254 nm. (b) With FeL_p, for preparative purposes, a solution in CH_2Cl_2 (ca. 500 mL, OD (254 nm)/cm ≈ 3) was irradiated at ambient temperature with the light of the Hg lamp using a quartz immersion well apparatus. During the photolysis (≈10 min, which corresponded to a conversion of ≈90%), the solution was stirred vigorously and a slight overpressure of dry argon was used to prevent atmospheric moisture from entering the solution. The solvent was then removed under vacuum, employing a trap cooled with liquid N_2 to avoid contact with water. After solvent removal, a black-bluish powder was recovered which consisted (on the basis of Mössbauer data, to ≥90%, in agreement with elemental analysis) of the one-electron oxidized complex $FeL_p]^{\bullet+}Cl^-$. Removal of solvent decreased the radical content only slightly, as judged by EPR and UV/vis spectroscopy. The powder ($FeL_p]^{\bullet+}Cl^-$) was found to be stable for ≥1 year when stored under dry air at room temperature. Efforts to purify $FeL_p]^{\bullet+}Cl^-$ by removal of unreacted FeL_p or to grow crystals of $FeL_p]^{\bullet+}$ as a Cl^-, PF_6^-, ClO_4^-, or Ph_4B^- salt for X-ray crystallography failed. Quantum yields were measured using ferrioxalate actinometry.[29]

Laser Photolysis Experiments. The excimer laser used (Lambda Physik EMG103MSC) produces ≈20-ns pulses of 248-nm (KrF*; typically 2 × 10^{16} to 1 × 10^{17} quanta/cm^2 per pulse at the position of the cell as measured using an Argon-saturated aqueous solution of KI for actinometry, taking $\Phi(e^-_{aq})$ from 248-nm photolysis to be 0.29[30]) or 193-nm (ArF*; 5 × 10^{15} to 1 × 10^{16} quanta/cm^2 per pulse) light. For experiments designed for product analysis, the solutions (OD/cm ≤ 1 at 248 nm) were photolyzed in 1 × 1 × 3 cm quartz cells. For the time-resolved measurements with optical and conductance detection, the solutions had OD/cm ≈ 1 at the excitation wavelengths 248 or 193 nm. They were flowed through the 2 mm (in the direction of the laser beam) × 4 mm (in the direction of the analyzing light) Suprasil quartz cell with typical rates of 1–2 mL/min, at a pulse repetition rate of ≈0.5 Hz. The pulse-induced time-dependent transmission and conductance changes were digitized with Tektronix 7612 and 7912 transient recorders interfaced with a DEC LSI 11/73$^+$ computer, which also controlled the other functions of the instrument and pre-analyzed the data. The data were further analyzed and stored on a VAX/VMS computer system.

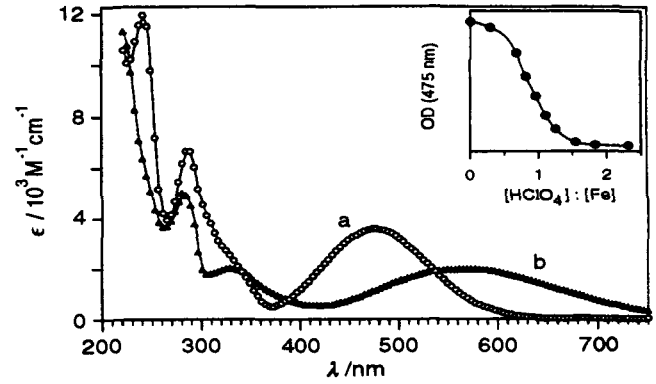

Figure 1. UV/vis spectra of FeL_p(a) and of $Fe_2(L_pH)_2]^{2+}$ (b) in CH_3CN. The extinction coefficient is based on the iron concentration; i.e. in the case of b, it is not corrected for the dimer formation. The inset shows the optical density at 475 nm plotted versus the ratio $[HClO_4]$:$[FeL_p]$.

In the presence of additives ($K_2S_2O_8$, $Li_4P_2O_8$, NaCl, KBr, KI), their contributions to the OD of the solutions were typically ≤30%. All photolysis experiments were performed at room temperature (≈20 °C).

Mössbauer and Resonance Raman Measurements. Mössbauer measurements were performed on powder samples of FeL_o, FeL_p, $Fe_2(L_pH)_2]^{2+}$, and $FeL_p]^{\bullet+}$ by using a transmission spectrometer of the constant acceleration type equipped with a $^{57}Co/Rh$ single-line source at room temperature. The temperature of the samples, which were mounted in an Oxford cryostat, was 4.2 K.

Resonance Raman (RR) measurements were performed at room temperature with excitation with the 468- and 568-nm lines of a Kr^+ laser (Model 171, Spectra Physics). The excitation wavelengths match the phenolate-to-Fe charge-transfer (ArOFe CT) bands. An optical multichannel detection system (Triplemate 1877, Spex Instruments, equipped with an O-SMA intensified diode array, Spectroscopy Instruments) was used. The spectral resolution was about 4.5 (4.0) cm^{-1}, and the resolution/diode, 1.0 (0.8) cm^{-1} at 482 (568) nm. The samples (OD/cm at the excitation wavelengths ≈ 0.5–2) were placed in a rotating cell to avoid laser-induced heating or photodamage. The laser power at the sample was about 25–50 mW focused by a 10-cm lens. No changes were observed in the RR spectra during the accumulation period (about 1 h), which indicates that the samples did not decompose. This is in agreement with the observation that the absorption spectra measured before and after the RR experiments were the same. A rapid photodecomposition, however, the observed for $FeL_p]^{\bullet+}$ upon excitation at 358 nm.

Results and Discussion

1. Absorption Spectra of Fe^{III}[1,4,7-tris(5-*tert*-butyl-2-oxybenzyl)-1,4,7-triazacyclononane] (FeL_p) and Fe^{III}[1,4,7-tris(3-*tert*-butyl-2-oxybenzyl)-1,4,7-triazacyclononane] (FeL_o) and Formation of Protonated Forms $Fe_2(L_pH)_2]^{2+}$ and $Fe(L_oH)]^+$. The structure of FeL_p, in which the iron is coordinated by a N_3O_3 donor set, has been determined by X-ray crystallography[27] (see Chart I, in which the ortho isomer, FeL_o, is also shown).

a. FeL_p. Figure 1a displays the UV/vis spectrum of FeL_p in acetonitrile. An essentially identical spectrum was observed in CH_2Cl_2 (see Figure 5a). There are three bands, at 242, 287, and 474 nm, and a shoulder near 330 nm. An additional, high-intensity band (not shown) is centered around 203 nm ($\epsilon = 5.5 \times 10^4$ M^{-1} cm^{-1}).

In order to assign the bands, the UV spectra of 2-methyl-4-*tert*-butylphenol, a model compound for the ligand, were recorded

(26) Metal complexes containing a phenol moiety as ligand have previously been oxidized: Kompan, O. E.; Ivakhnenko, E. P.; Lyubchenko, S. N.; Olekhnovich, L. P.; Yanovskii, A. I.; Struchkov, Y. T. *J. Gen. Chem. USSR* (*Engl. Transl.*) **1990**, 1682. However, these systems were not characterized structurally.

(27) Auerbach, U.; Eckert, U.; Wieghardt, K.; Nuber, B.; Weiss, J. *Inorg. Chem.* **1990**, *29*, 938.

(28) Auerbach, U.; Weyhermüller, T.; Wieghardt, K.; Nuber, B.; Bill, E.; Butzlaff, C.; Trautwein, A. X. *Inorg. Chem.* **1993**, *32*, 508.

(29) Murov, S. L. *Handbook of Photochemistry*; Dekker: New York, 1973.

(30) Jortner, J.; Levine, R.; Ottolenghi, M.; Stein, G. *J. Phys. Chem.* **1961**, *65*, 1232.

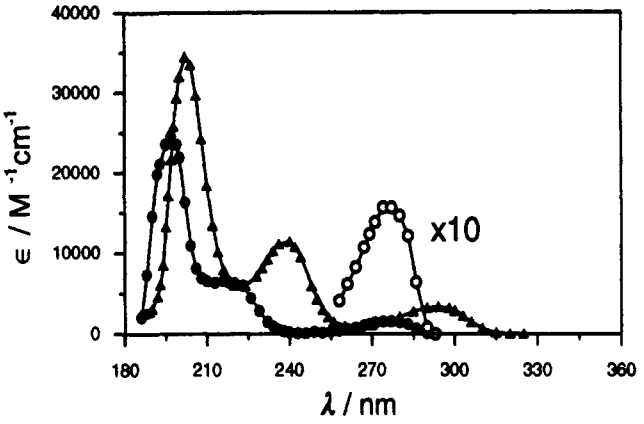

Figure 2. Absorption spectra of 2-methyl-4-*tert*-butylphenol in water at pH 3.8 (circles) and of the corresponding phenolate at pH 12 (triangles).

Chart I

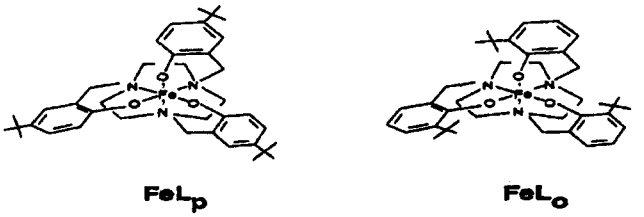

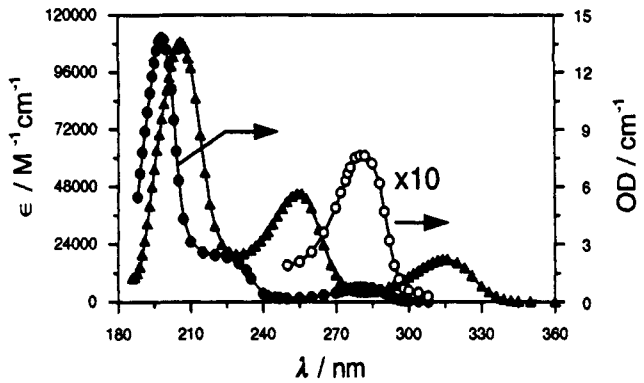

Figure 3. UV spectra in acetonitrile of L_p^{3-} in the presence of 10 mM *n*-$Bu_4N^+OH^-$ (triangles) and of a saturated solution of H_3L_p (circles).

in water at pH 3.8 (where the phenol OH is undissociated) and at pH 12 (where the OH group is ionized). The spectra are shown in Figure 2. 2-Methyl-4-*tert*-butylphenol exhibits three absorption bands, at 197, 225, and 280 nm. By analogy to the benzene transitions $^1E_{1u} \leftarrow {}^1A_{1g}$, $^1B_{1u} \leftarrow {}^1A_{1g}$, and $^1B_{2u} \leftarrow {}^1A_{1g}$, these bands can be assigned as π–π^* transitions.[31] It is evident that, upon deprotonation of the phenol, the bands undergo a bathochromic shift with a concomitant pronounced increase in their extinction coefficients.

The UV spectrum of the ligand, dissolved as the salt K_3L_p, could be obtained only in acetonitrile. In water, its solubility is not sufficient for obtaining a satisfactory signal. The spectrum of K_3L_p (Figure 3) is almost identical to that of *un-ionized* 2-methyl-4-*tert*-butylphenol, from which it is concluded that the ligand is present in acetonitrile in the protonated (neutral) form, i.e., as H_3L_p, apparently formed by reaction of traces of acid or water with the trianion, L_p^{3-}. In agreement with this is the fact that the absorption spectrum of the ligand did not change on addition of an excess of the strong acid $HClO_4$. In order to obtain the ligand in the anionic form, ≈0.1 mM K_3L_p was dissolved in acetonitrile containing 10 mM *n*-$Bu_4N^+OH^-$. The resulting spectrum, shown in Figure 3 (triangles), differs from that of the neutral form in a way analogous to the case of 2-methyl-4-*tert*-butylphenol and is therefore assigned to the trianion, L_p^{3-}. With L_p^{3-}, the bands (at 208, 254, and 315 nm) are red-shifted by ≥10 nm compared to those of 2-methyl-4-*tert*-butylphenolate in water, and the extinction coefficients are larger by approximately a factor of 3, as expected since the ligand contains *three* phenolates.

When the spectrum of L_p^{3-} is compared with that of FeL_p (Figure 1a), it is evident that by coordination of the phenolates to Fe(III), their π–π^* bands are shifted to lower wavelengths by an extent similar to that observed on protonation. This indicates that σ-bond formation between the oxygen lone pairs and Fe(III) leads to a reduced conjugation with the phenol ring.[32] The FeL_p band at 474 nm is due to the charge transfer (CT) $p_\pi \rightarrow d_\pi^*$ from the phenolate oxygen to the iron (ArOFe CT).[27,33-36] The shoulder near 330 nm is tentatively assigned to an amine-to-Fe CT transition.

Addition of $HClO_4$ to solutions of FeL_p in CH_3CN, CH_3OH, CH_2Cl_2, or acetone leads to systematic changes of its UV/vis spectrum (Figure 1b), with isosbestic points observed at 228, (271), 341, 389, and 538 nm. Quantitative analysis of the correlation between $[H^+]$ and the spectral changes shows that one proton is consumed per FeL_p (see inset of Figure 1). On addition of OH^-, the original spectrum is regenerated, demonstrating that the protonation reaction (eq 1) is reversible. The protonated species has been identified by X-ray crystallography and magnetic susceptibility measurements to be the dimer $Fe_2(L_pH)_2]^{2+}$, in which two FeL_p molecules are connected by two O–H···O hydrogen bonds (identical subunits).[27] The X-ray crystallographic data show that there are *three different* phenolate C–O bond lengths,[28] due to (a) a nonprotonated ($-O^-$), (b) a protonated (–OH), and (c) a nonprotonated but H-bonded ($O^-\cdots H$, involved in dimer formation) phenolate. The C–O bond length of the phenolate which is not involved in hydrogen bonding (type a, 1.334 Å) is essentially unchanged compared to that of the monomer (FeL_p, 1.323 Å) while the bond lengths of the hydrogen-bonded phenolates (types b and c) are increased to 1.392 and 1.374 Å, respectively. A schematic representation of the dimer emphasizing the different types of O···H···O bonds is depicted below:

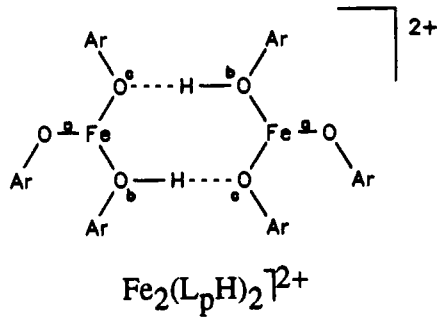

If the same species exists in solution, the spectrum shown in Figure 1b is that of $Fe_2(L_pH)_2]^{2+}$, and the reaction can be written as:

$$2FeL_p \underset{-2H^+}{\overset{+2H^+}{\rightleftharpoons}} [FeL_pH_2L_pFe]^{2+} (\equiv Fe_2(L_pH)_2]^{2+}) \quad (1)$$

Addition of ca. 10 vol % water to a solution of FeL_p and perchloric acid in the concentration ratio 1:2 in CH_3CN, MeOH, or acetone shifts the equilibrium (eq 1) quantitatively to the monomer side. This effect is obviously due to competition for the

(31) Jaffe, H. H.; Orchin, M. *Theory and Applications of Ultraviolet Spectroscopy*; Wiley: New York, 1962; pp 242–259.

(32) Gaber, B. P.; Miskowski, V.; Spiro, T. G. *J. Am. Chem. Soc.* **1974**, *96*, 6868.

(33) Flassbeck, C.; Wieghardt, K. *Z. Anorg. Allg. Chem.* **1992**, *608*, 60.

(34) Ainscough, E. W.; Brodie, A. M.; Plowman, J. E.; Brown, K. L. *Inorg. Chem.* **1980**, *19*, 3655.

(35) Patch, M. G.; Simolo, K. P.; Carrano, C. J. *Inorg. Chem.* **1983**, *22*, 2630.

(36) Spartalian, K.; Carrano, C. J. *Inorg. Chem.* **1989**, *28*, 19.

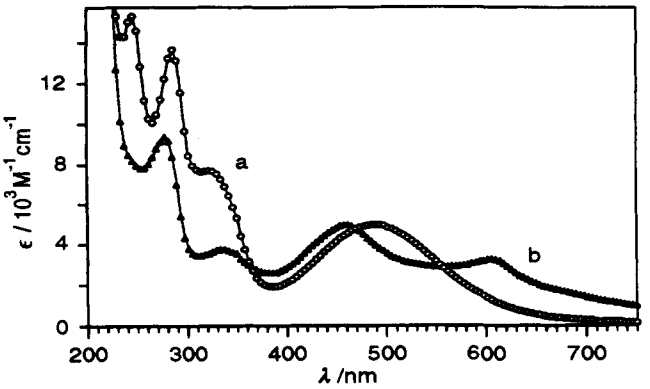

Figure 4. UV/vis spectra of FeL_o (a) and of $Fe(L_oH)]^+$ (b) in CH_3CN. The extinction coefficients ϵ are based on the iron concentration.

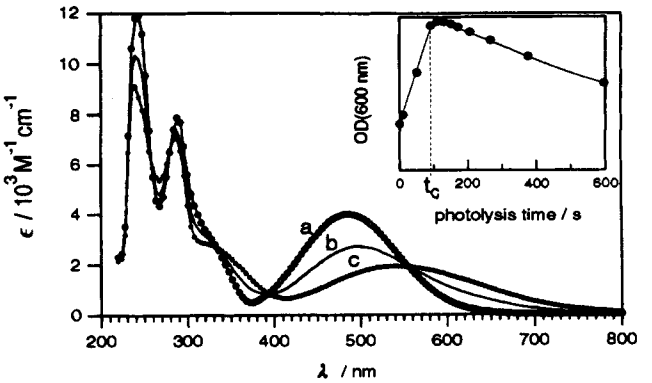

Figure 5. Effect of 254-nm photolysis on the UV/vis spectrum of FeL_p (≈0.2 mM) in CH_2Cl_2: (a) before photolysis, (b) after 45 s, and (c) after 90 s. The optical density of the parent solution (a) at 254 nm was 1.9 cm^{-1}. The inset shows the time-dependence of the optical density at 600 nm.

protons by the basic water molecules; i.e., water reduces the activity of the proton (leveling effect).[37]

The pentacoordinate complexes 4-RC_6H_4OFe(SALEN) (R = CH_3, Cl, CN; SALEN = *N,N'*-disalicylideneethylenediamine), the structure of which is shown below, have been studied in organic solvents using RR and UV/vis spectroscopy.[38,39] They are used here as models for the changes occurring in the ArOFe CT band of FeL_p upon protonation. With 4-RC_6H_4OFe(SALEN) it was found that, on going from R = CH_3 to Cl to CN, i.e., on decreasing the electron density of phenolate, the wavelengths of the $RC_6H_4O \rightarrow$ Fe CT bands *de*crease, whereas those of the *SALEN* → Fe CT bands *in*crease. Both phenomena can be understood in terms of the electronic effect of the substituents (and thus of the individual ligand(s)) remaining *localized*, in contrast to being (fully) transduced through the Fe(III). On this basis, the decrease to *lower* wavelengths (higher energies) in the $RC_6H_4O \rightarrow$ Fe CT bands reflects the lower electron densities of the phenolate (making the CT transition energetically more difficult), whereas the shift to *higher* wavelengths in the *SALEN*-phenolate-to iron transition is due to the increase of electron deficiency of Fe(III) as R in RC_6H_4O is varied from CH_3 to CN, in conjunction with the electron density of the *SALEN*-phenolates remaining approximately constant. If this is the case, electron donation from these phenolates to the "activated" (by RC_6H_4O) Fe becomes energetically easier; i.e., the CT band shifts to lower energies (higher wavelengths).

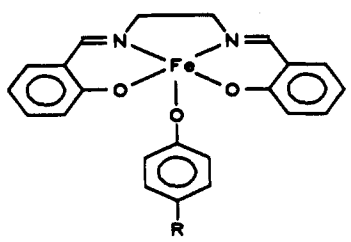

4-RC_6H_4O-Fe(SALEN)

The changes in the UV/vis spectrum of FeL_p occurring upon protonation (Figure 1) can be understood in an analogous way: In the proton-bridged dimer $Fe_2(L_pH)_2]^{2+}$, the electron density of the phenolates involved in the hydrogen bonding (types b and c) is reduced, making the CT transition energetically more difficult (blue shift of the band). The increase in the absorption at ≈370 nm (see Figure 1) is indicative of such a shift.[40] In comparison, the *red* shift of the CT band of the dimer compared to that of the monomer (by ≈90 nm) is a result of the increaseed electron deficiency of Fe(III) (resulting from protonation). In conjunction with an unchanged electron density of the two phenolate-groups of the dimer which are *not* involved in the hydrogen bond (type a), the increase in electron deficiency of the iron makes the CT transition energetically easier. As will be shown in section 5, this interpretation is supported by the results of RR measurements on FeL_p and $Fe_2(L_pH)_2]^{2+}$.[41] In comparison with FeL_p, the splitting into two components of the phenolate-to-iron CT band by protonation is much more clearly visible with FeL_o (see Figure 4).

From an inspection of Figure 1 it is evident that by protonation of FeL_p the two "ligand phenolate bands" (at 242 and 287 nm) are decreased in intensity and shifted toward lower wavelengths, an effect which is exactly analogous to what happens on protonation of uncomplexed phenolates (see Figures 2 and 3) and which is due to the resulting decrease in electron density.

b. FeL_o. In the case of FeL_o (for the spectrum, see Figure 4a), addition of $HClO_4$ leads to changes (not shown) in the UV/vis spectrum which are qualitatively similar to those observed for $FeL_p/Fe_2(L_pH)_2]^{2+}$. However, on the basis of titrimetric data, only *one* proton is consumed for every *two* Fe atoms. This can be explained in terms of formation of a singly proton-bridged dimer $H(FeL_o)_2]^+$. Further addition of acid results in a species with the ArOFe CT band split into two components at 459 and 606 nm with extinction coefficients of ca. 4850 and 3220 M^{-1} cm^{-1}, respectively (Figure 4b). On the basis of titrimetric data, this spectrum is attributed to the protonated monomer, $Fe(L_oH)]^+$. In analogy to the interpretation of the UV/vis spectra given for the case of FeL_p, the absorption band at 459 nm (Figure 4b) is assigned to the ArOFe CT of the protonated phenolate groups involved in the hydrogen bridge (types b and c), and the long wavelength component (606 nm) to that of the *non*-hydrogen-bonded phenolate (type a). The RR results support this interpretation (see section 5).[39]

2. Effects of Photolysis on Absorption Spectra. Formation of Oxidized Species. a. Photolysis with Light of 254 nm. Figure 5 displays the UV/vis spectrum of FeL_p in CH_2Cl_2 (a) and the spectral changes occurring upon photolysis with the 254-nm line of the Hg lamp (b,c). As shown in the inset, at λ = 600 nm the optical density (OD) increases steeply with photolysis time to

(37) While being cooled from ambient temperature to 77 K, the equilibrium (in the solvent 2-methyl-tetrahydrofuran) is shifted in favor of the monomeric form.

(38) Pyrz, J. W.; Roe, A. L.; Stern, L. J.; Que, L. *J. Am. Chem. Soc.* **1985**, *107*, 614.

(39) The resonance enhancement of Raman bands was measured for different excitation wavelengths (excitation profiles).[38] On this basis, it was possible to individually identify the SALEN and RC_6H_4O-to-Fe CT bands.

(40) With the dimer $Fe_2(L_pH)_2]^{2+}$, there is a band at 330 nm (Figure 1). This could, in principle, be due to the types b and c phenolate-to-Fe CT transition. However, at this position there is also the presumed N–Fe CT band. It is therefore difficult to unambiguously assign this 330-nm band.

(41) However, as revealed by the RR experiments, the long-wavelength-absorption band also includes small degrees of admixture of the CT transition of the hydrogen-bonded phenolates.

Table I. Quantum Yields Φ for the Decomposition of FeL_p and FeL_o in CH_2Cl_2[a] as a Function of λ(excitation)

λ/nm	Φ (para)	Φ (ortho)
248	0.3	0.1
254	0.2	0.1
290	<0.01	<0.01
300	<0.005	<0.005

[a] Monitored via the OD increase at 600–620 nm.

reach a maximum at ≈100 s, after which there is a slow decrease upon further irradiation. Up to photolysis times ≈100 s, isosbestic points are observed (at 258, 280, 335, 392, and 555 nm). For the spectra 5c (isosbestic points still well defined) and 5a, the ratio of the optical densities at 474 nm is 0.35:1. If only the parent compound FeL_p did absorb at 474 nm, the value (1–0.35): 0.35 = 1.86 would give the ratio [product]/[FeL_p] (assuming equal extinction coefficients). Assuming that the photoproduct has a nonzero absorption at 474 nm, the value 1.86 is a lower limit for [product]/[FeL_p]. However, from Mössbauer measurements on $FeL_p]^{\bullet+}$ (see section 3) the lower limit for this ratio is 9. On this basis, ≥90% of the parent have been converted at t_c, and the spectrum observed (Figure 5c) can be regarded as being essentially that of the product ($FeL_p]^{\bullet+}$, see later). Analogous results were obtained in the case of FeL_o and in other chloroalkanes such as $ClCH_2Cl_2Cl$, *n*-butyl chloride, or *sec*-butyl chloride. In contrast, in acetonitrile or alcohols, the complexes FeL_p or FeL_o were found to be photo*stable*.

The quantum yields for the photodecomposition of FeL_p indicated in Table I were estimated by assuming that the spectrum obtained at 90-s photolysis time is that of the product $FeL_p]^{\bullet+}$. The quantum yields are strongly wavelength-dependent: They are significantly lower for the $^1B_{2u} \leftarrow {}^1A_{1g}$ transition (≈290 nm) than for the $^1B_{1u} \leftarrow {}^1A_{1g}$ transition (≈250 nm).

b. Laser Flash Photolysis. Solutions of FeL_p (≈40 μM) in air-saturated chloroalkanes in 1 × 1 × 3 cm Suprasil quartz cells were photolyzed with the pulsed 248-nm laser light, and the photoinduced spectral changes were recorded with a spectrophotometer. The changes were found to be the same as those induced with the Hg lamp (see Figure 5). In the absence of moisture, the spectra did not change within several hours after photolysis. The amplitudes of the absorption changes of these solutions (e.g., at 475 and 600 nm) were proportional to the intensity of the laser pulses (varied by filters) up to photon fluxes of 10^{25} cm^{-2} s^{-1}. Furthermore, it was found that, compared to the effect of the 254-nm light (Hg lamp), the same number of photons produce similar spectral changes. This indicates that the spectral changes result from a monophotonic reaction.

Time-resolved studies were also performed. In Figure 6b is shown the spectrum observed on photolysis of FeL_p in CH_2Cl_2 with 20-ns pulses of the 248-nm laser light. Negative optical density changes centered at 242 and 478 nm are seen (due to depletion of parent), and positive ones at 269, 370, and 620 nm (indicating formation of product). The spectral changes, which are qualitatively similar to those obtained with the low-intensity light of the Hg lamp (spectra b and a of Figure 6), remained constant from 20 ns to 400 μs after the pulse.[42] Ar- and O_2-saturated solutions gave exactly the same results, showing that O_2 has no influence on the photoreaction. The amplitude of the optical changes was found to be proportional to the laser power, further support for the monophotonic reaction reported above. DC-conductance detection was also used. An instantaneous increase of the conductance was observed after the pulse which remained constant (no decay up to 400 μs after the pulse). The conductance increase demonstrates the production of ions.

When *non*chlorinated hydrocarbons such as CH_3CN, CH_3OH, 2-propanol, cyclohexane, dioxane, trifluoroethanol, or CH_3CN/H_2O mixtures were employed, 248-nm photolysis of $FeL_{p/o}$ resulted in only very weak changes in the spectra, indicating that the complexes are essentially stable in these solvents. However, with excitation at 193 nm (ε(193 nm) = 3.4×10^4 M^{-1} cm^{-1}, $^1E_{1u} \leftarrow {}^1A_{1g}$ transition) in CH_3CN, spectra similar to those in CH_2Cl_2 were observed (spectrum 6c), but the species formed decayed rapidly. The decay could be inhibited by the addition of small amounts of electron scavengers such as, e.g., 0.7 vol %, CH_2Cl_2. This implies that the decay of the photoproduct is due to recombination with solvated electrons.

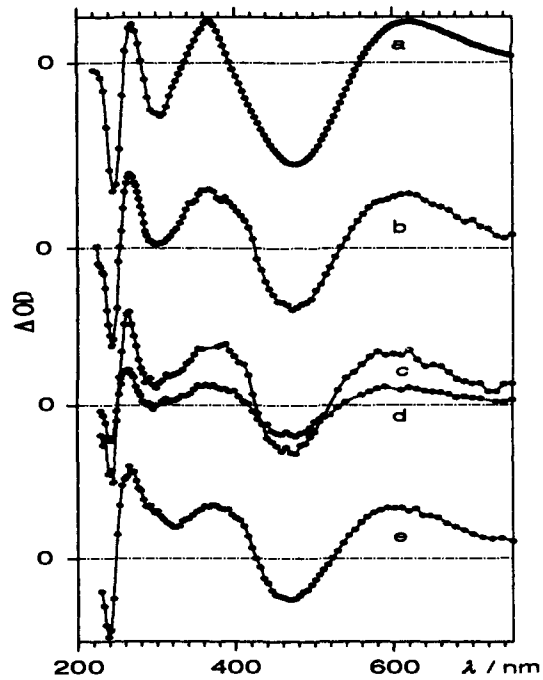

Figure 6. ΔOD spectra obtained with FeL_p: (a) difference between spectra c and a of Figure 5 (photolysis in CH_2Cl_2 with 254-nm light); (b) spectrum obtained by laser photolysis of FeL_p (44 μM) in CH_2Cl_2 with light of 248 nm (recorded 70 ns after the end of the pulses); (c) spectra obtained by laser photolysis of FeL_p (30 μM) in CH_3CN with 193-nm light measured 400 ns, and (d) 20 μs after the pulse; (e) spectrum recorded after reaction of $SO_4^{\bullet-}$ radicals ($[SO_4^{\bullet-}]_{t\to 0} \ll$ [Fe]) in 3:1 v:v CH_3CN/H_2O. The $SO_4^{\bullet-}$ radicals were produced by 248-nm laser photolysis in the presence of $K_2S_2O_8$ (≈20 mM).

c. Reaction with Oxidizing Radicals. As shown in Figure 6e, difference spectra similar to those of a, b, and c of Figure 6 were obtained by reaction of FeL_p with $SO_4^{\bullet-}$.[43] This radical was produced in the presence of FeL_p in CH_3CN/H_2O mixtures by 248-nm photolysis of $S_2O_8^{2-}$, which leads to homolytic cleavage of the peroxide bond:

$$S_2O_8^{2-} \xrightarrow{h\nu} 2SO_4^{\bullet-} \qquad (2)$$

Under these conditions, FeL_p (and FeL_o) are photochemically completely inert. Since the $SO_4^{\bullet-}$ radical typically reacts by one-electron transfer,[44,45] the product of its reaction with FeL_p (k = 3.5×10^9 M^{-1} s^{-1} in 3:1 (v:v) CH_3CN/H_2O) is likely to be the corresponding radical cation, $FeL_p]^{\bullet+}$:

$$SO_4^{\bullet-} + FeL_p \rightarrow SO_4^{2-} + FeL_p]^{\bullet+} \qquad (3)$$

$FeL_p]^{\bullet+}$ was also generated by addition of the strong oxidant O_2AsF_6 to a solution of FeL_p in CH_2Cl_2. However, as judged by

(42) At longer times, the OD changes were not monitored, due to incipient instabilities of the analyzing light.

(43) The phosphate radical $H_2PO_4^{\bullet}$ has a reactivity similar to that of $SO_4^{\bullet-}$, whereas the anionic forms $HPO_4^{\bullet-}$ and $PO_4^{\bullet 2-}$ (see: Maruthamuthu, P.; Neta, P. *J. Phys. Chem.* **1978**, *82*, 710) are not sufficiently reactive with FeL_p.

(44) Eberson, L. *Electron Transfer Reactions in Organic Chemistry*; Springer: Berlin, 1987.

(45) Steenken, S. In *Free Radicals in Synthesis and Biology*; Minisci, F., Ed.; NATO ASI Series C260; Kluwer: Dordrecht, The Netherlands, 1989; p 213.

the UV/vis spectrum of the resulting solution, the product was less pure than that from the photolysis in CH_2Cl_2.[46]

d. The Photochemical Reaction and the Structure of $FeL_{p/o}]^{\bullet+}$. On the basis of the spectroscopic data presented above, and in agreement with the photoinduced conductance increase observed, it is evident that the complexes FeL_p and FeL_o, if present in chlorinated hydrocarbons (RCl), are ionized by photolysis with light of 248 nm (quantum energy 5.0 eV) or 254 nm (4.9 eV, $^1B_{1u} \leftarrow {}^1A_{1g}$ transition). The ionization process (eq 4) requires only

$$FeL_{p/o} \xrightarrow[\lambda_{exc} = 248/254\ nm]{h\nu} FeL_{p/o}{}^{*} \xrightarrow{+RCl} FeL_{p/o}]^{\bullet+} + R^{\bullet} + Cl^{-} \quad (4)$$

$$FeL_{p/o} \xrightleftarrows{CH_3CN,\ h\nu = 193\ nm} FeL_{p/o}]^{\bullet+} + e^{-}_{solv} \quad (5)$$

$$e^{-}_{solv} + RCl \rightarrow R^{\bullet} + Cl^{-} \quad (6)$$

one photon. Interestingly, with solvents other than RCl, even if they are much more polar (such as acetonitrile) and therefore more supportive of charge separation, ionization does *not* take place. This may be interpreted on the basis of a very short-lived ($\leq$1 ps) excited-state $FeL_{p/o}$* which is irreversibly scavenged via dissociative electron transfer to RCl, yielding $FeL_p]^{\bullet+}$, R•,[47] and Cl^- (eq 4), whereas in solvents which do *not* have irreversible electron-scavenging abilities there is essentially quantitative loss of the excitation energy by internal conversion to the ground state.

With the high quantum energy of 193-nm light (6.4 eV, $^1E_{1u} \leftarrow {}^1A_{1g}$ transition of the phenolate ligands), ionization is possible in CH_3CN (eq 5). Solvated electrons formed were not *directly* detected, which is not surprising since their absorption in CH_3CN is small[48] compared to the absorption changes due to the oxidation of $FeL_{p/o}$. However, evidence for photoejected electrons is the decay of $FeL_{p/o}]^{\bullet+}$ (see Figure 6c,d) in the *absence* of electron scavengers, which is assigned to recombination of solvated electrons with $FeL_{p/o}]^{\bullet+}$ (leading to recovery of $FeL_{p/o}$).

It is very interesting that the spectrum of $FeL_p]^{\bullet+}$ (see Figure 5c) is very similar to that of the dimer $Fe_2(L_pH)_2]^{2+}$ (Figure 1b). In particular, both spectra exhibit a long-wavelength absorption ($\approx$600 nm), which is responsible for the blue color of solutions of the dimer and of $FeL_p]^{\bullet+}$. The long-wavelength absorption of the *dimer* was assigned to the CT transition involving the type a phenolates (see section 1a), arguing that the increased electron deficiency of Fe(III) resulting from protonation of the type b and c phenolates lowers the energy of the type-a-phenolate-to-Fe transition. If it is assumed that the oxidation of FeL_p involves transformation of an (electron-rich) phenolate ligand into an (electron-deficient) phenoxyl radical,[49] with a weakened coordination to Fe(III), this electron deficiency would have the same effect as that produced by protonation in the case of the dimer. On this basis, the long-wavelength absorption band of $FeL_{p/o}]^{\bullet+}$ can be assigned to the ArO-Fe CT of the two remaining phenolates. Concerning the π–π* bands of the ligand phenolates, oxidation leads to a decrease of the extinction coefficients and of the λ_{max} values in a way similar to that observed on protonation (compare Figures 1 and 5).

In addition to the positive ΔOD values at wavelengths above ca. 520 nm observed on transforming FeL_p into $FeL_p]^{\bullet+}$, the spectra of Figures 5 and 6 show positive values near 270 and 370 nm. Phenoxyl radicals, connected by an ortho methylene bridge to an ammonium nitrogen and hydrogen-bonded to this nitrogen (six-membered-ring configuration), exhibit absorption bands in these regions.[13] Therefore, by analogy it is suggested that the positive OD changes observed around 370 and 270 nm are due to the phenoxyl group bonded to Fe(III). On the basis of this analysis of the optical spectra,[50] which is supported by the results of RR measurements (see section 5) and is in line with the data from Mössbauer (see section 3) studies, the structure of $FeL_{p/o}]^{\bullet+}$ can be described as a complex in which Fe(III) is coordinated by two phenolates and one phenoxyl group, formed by removal (via photoionization or electron transfer to an oxidant) of an electron from one of the phenolates, as shown in eq 7.

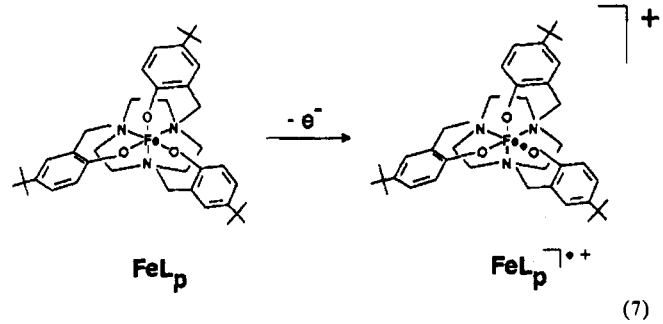

(7)

Table II. Mössbauer Parameters of ^{57}FeL Compounds at 4.2 K

	isomer shift relative to α-Fe in mm/s	quadrupole-splitting in mm/s
FeL_o	0.386	0.896
FeL_p	0.385	0.549
$Fe_2(L_pH)_2]^{2+}$	0.399	1.061
$FeL_p]^{\bullet+}$	0.420	0.892

3. Mössbauer Spectroscopy. Samples of FeL_p, $Fe_2(L_pH)_2]^{2+}$, and $FeL_p]^{\bullet+}$ and of FeL_o in powder form with the natural distribution of isotopes (2% ^{57}Fe) were used for Mössbauer measurements at 4.2 K. In the case of $FeL_p]^{\bullet+}$, the signal-to-noise ratio was such that a contamination of 10% of FeL_p would have been detected. Since FeL_p was not observed, it is concluded that the $FeL_p]^{\bullet+}$ sample contained less than 10% of the parent. The isomer shifts and quadrupole splittings determined for FeL_p, $Fe_2(L_pH)_2]^{2+}$, $FeL_p]^{\bullet+}$, and FeL_o are listed in Table II.

Concerning the isomer shifts, their values (0.38–0.42) fall in the range 0.3–0.6 mm s^{-1}, which is characteristic for mononuclear octahedral high-spin ^{57}Fe(III) complexes.[51–55] In comparison, values for ^{57}Fe(IV) are typically in the range –0.2 to +0.2 mm s^{-1}.[56–59] The conclusion is thus that upon oxidation of $FeL_{p/o}$ (eq 4 and 7) *no* Fe(IV) species are formed. The low values for Fe(IV) compared to Fe(III) are due to the fact that conversion of Fe(III)

(46) Oxidants such as the dihalogen radical anions $Cl_2^{\bullet-}$, $Br_2^{\bullet-}$, and $I_2^{\bullet-}$ were found not to lead to oxidation of FeL_p, although there was some reactivity.

(47) The alkyl radicals are likely to disappear by dimerization or disproprotionation.

(48) Hirata, Y.; Mataga, N.; Sakata, Y.; Misumi, S. *J. Phys. Chem.* **1983**, *87*, 1493.

(49) The basicity of the phenoxyl radical is lower by 12 orders of magnitude than that of phenolate (as reflected by the fact that pK_a(phenol) = 10, but pK_a(phenol$^{\bullet+}$) = –2), see: Steenken, S. *Free Radical Res. Commun.* **1992**, *16*, 349.

(50) The optical data from experiments with mono- and bis(phenolato)iron(III) complexes support this picture.[13]

(51) Greenwood, N. N.; Gibb, T. C. *Mössbauer Spectroscopy*; Chapman and Hall: London, 1971.

(52) Murray, K. S. *Coord. Chem. Rev.* **1974**, *12*, 1.

(53) Spartalian, K.; Carrano, C. J. *J. Chem. Phys.* **1983**, *78*, 4811.

(54) Carrano, C. J.; Spartalian, K.; Appa Rao, G. V. N.; Pecoraro, V. L.; Sundaralingam, M. *J. Am. Chem. Soc.* **1985**, *107*, 1651.

(55) Kessel, S. L.; Emberson, R. M.; Debrunner, P. G.; Hendrickson, D. N. *Inorg. Chem.* **1980**, *19*, 1170.

(56) Gold, A.; Jayaraj, K.; Doppelt, P.; Weiss, R.; Chottard, G.; Bill, E.; Ding, X.; Trautwein, A. X. *J. Am. Chem. Soc.* **1988**, *110*, 5756 and references therein.

(57) Berry, F. J. In *Mössbauer Spectroscopy*; Rossiter, B. W.; Hamilton, J. F., Eds.; Physical Methods of Chemistry Vol. V; John Wiley and Sons: New York, 1990. Wegener, H. *Der Mössbauer-Effekt und seine Anwendungen in Physik und Chemie*; Bibliographisches Institut: Mannheim, Germany, 1965; pp 9–110 and 163–171.

(58) Mandon, D.; Weiss, R.; Franke, M.; Bill, E.; Trautwein, A. X. *Angew. Chem.* **1989**, *101*, 1747.

(59) Collins, T. J.; Kostka, K. L.; Münck, E.; Uffelman, E. S. *J. Am. Chem. Soc.* **1990**, *112*, 5637.

into Fe(IV) involves removal of a 3d electron. Since d electrons shield the nucleus from the s electrons, a decreasing d electron population leads to an increase in the s electron density at the nucleus. In ^{57}Fe, a higher s electron density at the nucleus leads to a reduction of the isomer shift.[57,60] Concerning the effect of protonation or oxidation, the decrease in the s electron density at the $^{57}Fe(III)$ nucleus as a result of the reactions involving the ligand is clearly visible by the increase of the isomer shift: With FeL_p, the isomer shift increases upon protonation, and it increases even more upon one-electron oxidation. This is strong support for the conclusions reached on the basis of the optical data concerning the structure and formation of $FeL_p]^{\bullet+}$ (see eq 7).

The quadrupole splitting is a measure of the asymmetry of the electrical charge distribution around the nucleus. As seen in Table II, for $Fe_2(L_pH)_2]^{2+}$, the quadrupole splitting is strongly enhanced relative to the parent compound FeL_p, indicating a decreased symmetry about the ^{57}Fe nucleus. This is as expected on the basis of the X-ray structure[27] of the dimer. In comparison to the symmetric monomer, FeL_p, the dimer has *three* types of phenolate, as described in Section 1a.

Also for $FeL_p]^{\bullet+}$, the quadrupole splitting is enhanced compared to that for FeL_p, reflecting increased asymmetry. In support of the conclusions described in section 1c and the data from RR measurements (section 5), this suggests that the hole (missing electron) is localized at *one* phenolate group in contrast to being delocalized over the three phenolates.[61,62]

4. Resonance Raman studies were performed using excitation at 482 and 568 nm. These wavelengths coincide with the ligand-to-metal CT transitions of the parent complexes and their protonated and radical forms, respectively. The charge transfer affects the Fe–O and the C–O bond lengths so that considerable resonance enhancement is expected for the Fe–O and C–O stretching vibrations. Furthermore, the latter mode and in particular the internal ring modes of the ligands may gain significant intensity via coupling to the lowest $\pi \rightarrow \pi^*$ transition of the phenolates which presumably mixes with the CT transition.[63] Such mixing would explain the high intensity of the 600-nm absorption band. Assignments of the observed Raman bands are based on the known Raman properties of model phenols and phenoxyl radicals,[63-69] in particular of 2,4- and 2,6-dimethylphenol.[64,65]

Concerning the parent compounds FeL_p and FeL_o, their strongest RR bands (see Figures 8–10) are in the region between 1000 and 1700 cm^{-1}, which includes the internal ring modes of the phenolate ligands as well as the C–O stretch vibrations (mode ν_{7a}). The latter mode gives rise to the bands at 1307 and 1299 cm^{-1} in FeL_p and FeL_o, respectively (Figures 9, 10). According to a previous study on a number of ferric phenolate complexes,[70] a frequency at $\approx$1305 cm^{-1} corresponds to a C–O bond length of about 1.32 Å, which agrees very well with the values obtained from the crystallographic analysis of FeL_p.[28] Above 1400 cm^{-1}, the RR spectra of both FeL_p and FeL_o are dominated by two bands which can be attributed to the modes ν_{8a} and ν_{19a} at 1606 (1587) and 1500 (1525) cm^{-1} in FeL_p (FeL_o). While the high intensity of the mode ν_{8a} is consistent with the view of a mixing between the CT and the lowest $\pi \rightarrow \pi^*$ transitions of the phenolates, the reason for the enhancement of the mode ν_{19a}, which in the RR spectra of phenolic compounds can hardly be detected, is not clear, in particular, since this mode does not include significant contributions from the C–O stretching.[71]

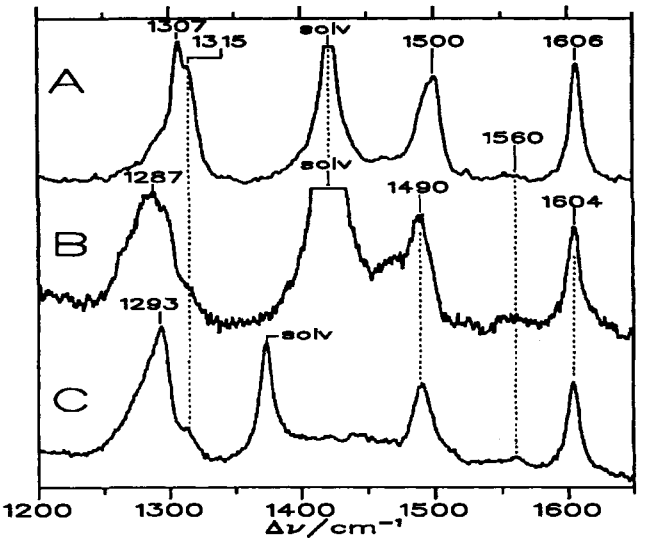

Figure 7. Resonance Raman spectra of FeL_p and $FeL_p]^{\bullet+}$ in CH_2Cl_2 and of $Fe_2(L_pH)_2]^{2+}$ in CH_3CN: (A) FeL_p, excited at 482 nm, (B) $FeI_p]^{\bullet+}$, excited at 568 nm, (C) $Fe_2(L_pH)_2$, excited at 568 nm.

The Fe–O stretching, however, is more difficult to identify, although in related Fe phenolate complexes, this mode (observed between 570 and 630 cm^{-1}, depending on the Fe–O bond length[38,70,72]) has been unambiguously assigned by isotopic labeling.[38] Figure 9A displays the RR spectrum of FeL_o in this spectral region. The weak but distinct peak at 601 cm^{-1} is assigned to the Fe–O stretching. An alternative assignment to an internal mode of the ligands is not very likely to be correct since the Raman spectra of 2-methyl-6-*tert*-butylphenol do not display any band in this region (spectra not shown). In the case of the para-substituted complexes an unambiguous assignment of the Fe–O stretching does not appear to be possible without isotopic labeling, although a very weak band at $\approx$600 cm^{-1} is observed for FeL_p, which corresponds to the expected value derived from the bond length–frequency correlation reported by Carrano et al.[70]

Upon protonation or oxidation, the RR spectra of FeL_p and FeL_o change appreciably (see Figures 7–9). Concerning the phenolate C–O bond, oxidation or protonation leads to a frequency *de*crease of the C–O stretching by up to 20 cm^{-1}, e.g., from $\approx$1312 for FeL_p to 1293 cm^{-1} for $Fe_2(L_pH)_2]^{2+}$, indicating an increase of the C–O bond length. In the case of $Fe_2(L_pH)_2]^{2+}$, the X-ray crystallographic data[28] show the presence of *three* different phenolate C–O bond lengths, as pointed out in section 1a. On this basis, the 1293-cm^{-1} RR band is assigned to the C–O stretching of the hydrogen-bonded phenolates (types b and c).

(60) Fe(II) compounds show isomer shifts increased by $\approx$0.9 mm s^{-1} relative to those for Fe(III) compounds.

(61) The validity of this statement concerning localization is restricted to the time scale inherent in the analytical method employed. With Mössbauer spectroscopy (quadrupole splittings), the time scale is 10^{-7} s. This means that if intramolecular proton transfer from phenol to phenolate (in the case of $Fe_2(L_pH)_2]^{2+}$) or electron transfer from phenolate to phenoxyl (in the case of $FeI_{p/o}]^{\bullet+}$) occurred, its rate would be $<10^7$ s^{-1}. The time scale of RR is $\approx 10^{-13}$ s.

(62) It is worth mentioning but presently not understood that the quadrupole splitting of FeL_o is as large as that for $FeL_p]^{\bullet+}$.

(63) Gaber, B. P.; Miskowski, V.; Spiro, T. G. *J. Am. Chem. Soc.* **1974**,
(64) Green, J. H. S.; Harrison, D. J.; Kynaston, W. *Spectrochim. Acta, Part A* **1972**, *28*, 33.
(65) Barnah, G. D.; Dube, P. S.; Singh, S.; Singh, S. R. *Indian J. Pure Appl. Phys.* **1972**, *10*, 302.
(66) Tripathi, G. N. R.; Schuler, R. H. *J. Phys. Chem.* **1988**, *92*, 5129. Tripathi, G. N. R. In *Time-Resolved Resonance Raman Spectroscopy of Chemical Reaction Intermediates in Solution*; Clark, R. J. H., Hester, R. E., Eds.; Advances in Spectroscopy Vol. 18; Wiley: New York, 1989; pp 157–215.
(67) Tomimatsu, Y.; Kint, S.; Scherer, R. J. *Biochemistry* **1976**, *15*, 4918.
(68) Tripathi, G. N. R.; Schuler, R. H. *J. Chem. Phys.* **1984**, *81*, 113.
(69) Dollich, F. R.; Fateley, W. G.; Bentley; F. F. *Characteristic Raman Frequencies of Organic Compounds*; Benzene and Its Derivatives; Wiley: New York, 1974; Chapter 13. Varsanyi, G.; Szoke, S. *Vibrational Spectra of Benzene Derivatives*; Academic Press: New York, 1979. Schrader, B.; Meier, W. *Raman/IR Atlas Organischer Verbindungen*; Verlag Chemie: Weinheim, Germany, 1974.
(70) Carrano, C. J.; Carrano, M. W.; Sharma, K.; Backes, G.; Sanders-Loehr, J. *Inorg. Chem.* **1990**, *29*, 1865.
(71) Harada, I.; Takeuchi, H. In *Spectroscopy of Biological Systems*; Clarke, R. J. H., Hester, R. E., Eds.; Wiley: New York, 1986; Vol. 13, pp 113–176.
(72) Nagai, M.; Yoneyama, Y.; Kitagawa, T. *Biochemistry* **1989**, *28*, 2418.

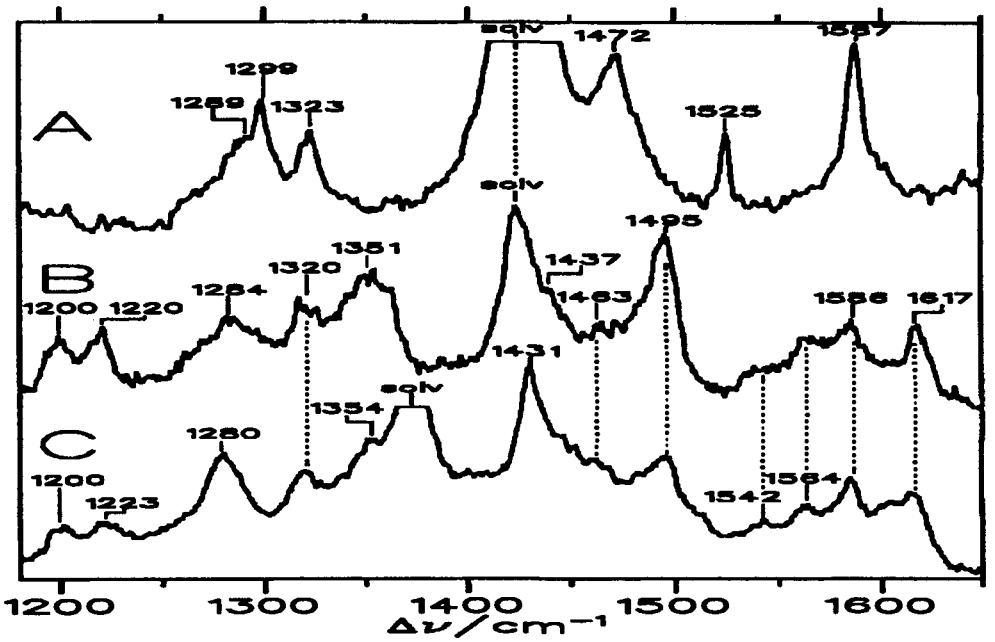

Figure 8. Resonance Raman spectra of FeL_o and $FeL_o]^{\bullet+}$ in CH_2Cl_2 and of $Fe(L_oH)]^+$ in CH_3CN: (A) FeL_o, excited at 482 nm, (B) $FeL_o]^{\bullet+}$, excited at 568 nm, (C) $Fe(L_oH)]^+$, excited at 568 nm.

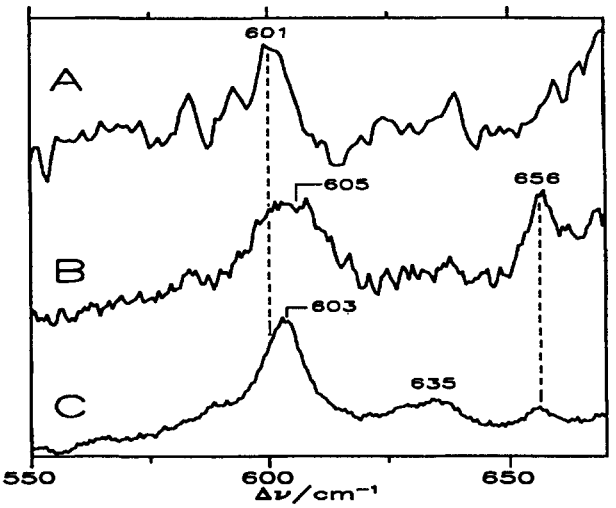

Figure 9. Resonance Raman spectra (Fe–O stretch vibrations) of FeL_o and $FeL_o]^{\bullet+}$ in CH_2Cl_2 and of $Fe(L_oH)]^+$ in CH_3CN: (A) FeL_o, excited at 482 nm, (B) $FeL_o]^{\bullet+}$, excited at 468 nm, (C) $Fe(L_oH)]^+$, excited at 568 nm.

Also, the other bands above 1400 cm^{-1} are likely to originate from the internal modes of the hydrogen-bonded phenolates. The frequency of the mode ν_{19a} has been shown[38] to change parallel to that of the C–O stretching. This would account for the 10 and 30 cm^{-1} downshifts in the para- and ortho-substituted complexes, respectively. Also, the downshift of the mode ν_{8a} fits into the picture, taking into account the sensitivity of this mode toward hydrogen bonding.[73]

Concerning the Fe–O bond, as pointed out above, the RR spectrum of $Fe_2(L_pH)_2]^{2+}$ contains no reliable information on the Fe–O stretch vibration. Attempts to understand the effect of protonation or oxidation on the Fe–O bond are therefore restricted to FeL_o. On the other hand, only in the case of the para system, $Fe_2(L_pH)_2]^{2+}$, are X-ray data available,[28] and these show that the Fe–O distance of the two phenolates which do not participate in the hydrogen bridges (–O⁻, type a, 1.861 Å) is shortened compared to the Fe–O distance in FeL_p (1.918 Å), whereas the Fe–O bond lengths of the protonated (–OH, type b) and O⁻···H (type c) phenolates are increased to 2.041 and 1.954 Å, respectively. In the Fe–O stretching region, the RR spectra of the three FeL_p species show a band at very similar frequencies, i.e., at ≈600 cm^{-1} (Figure 9). Thus it can be ruled out that in $Fe_2(L_pH)_2]^{2+}$ this band is due to the protonated phenolate ligand (type b) since the substantial increase of the bond length should be reflected by a significant frequency downshift of the Fe–O stretching.[70] However, if protonation affects this band at all, there is a small shift to higher frequencies. Thus we conclude that it is the Fe–O stretching of the type a phenolates which contributes to the observed RR band of $Fe_2(L_pH)_2]^{2+}$. This implies that excitation in resonance with the 600-nm transition leads to a preferential enhancement of the Fe–O vibrations of the type a phenolates while for the type b and c phenolates only the internal ligand modes are enhanced. From this it is concluded that the CT-transfer transition at 600 nm also includes contributions from the phenolate types b and c. Since the resonance enhancement is not sufficient to yield detectable bands of the Fe–O stretching of the phenolates b and c, the contributions of the CT of these ligands to the 600-nm bands are apparently small, which is in line with the findings discussed in Section 2c. The significant enhancement of the internal modes of these phenolates, however, may be due to the coupling of $\pi \rightarrow \pi^*$ transitions of these ligands with the corresponding CT transition. Apparently, this coupling is more efficient for the type b and c than for the type a phenolates since the RR spectra do not display any bands attributable to internal modes of the latter ligands.

A particularly interesting observation is that the RR spectra of the oxidized species, $FeL_p]^{\bullet+}$ or $FeL_o]^{\bullet+}$, and of the protonated species, $Fe_2(L_pH)_2]^{2+}$ or $Fe(L_oH)]^+$, are essentially the same (as is the case with the UV/vis spectra; see sections 1 and 2). This indicates that the removal of an electron has the same effect as the addition of a proton. Since the addition of a proton affects an *individual* phenolate rather than all phenolates collectively, the conclusion is thus that the hole (electron deficiency) is *localized* (on a phenolate) in contrast to being *de*localized over two or three phenolates. In $FeL_p]^{\bullet+}$ and $FeL_o]^{\bullet+}$, the Fe^{III} nucleus is thus coordinated by three nitrogens, two phenolates, and *one phenoxyl* ligand.[61]

5. Reactivity of $FeL_p]^{\bullet+}$. A few experiments were performed related to the chemical reactivity of $FeL_p]^{\bullet+}$. In the *dry* solvents CH_2Cl_2 and CH_3CN at ambient temperature, the oxidized

(73) Hildebrandt, P.; Copeland, R. A.; Spiro, T. G.; Otlewski, J.; Laskowski, M.; Prendergast, F. *Biochemistry* **1988**, *27*, 5426.

complexes $FeL_{p/o}]^{\bullet+}$ are stable for months. However, in the presence of moisture, they disappear relatively rapidly. E.g., if a drop of water is placed on the surface of a ≈0.1 mM solution of $FeL_p]^{\bullet+}$ in CH_2Cl_2, the blue color of the solution disappears in the course of ≈10 h and the parent compound's UV/vis spectrum is entirely regenerated. The same is true for solutions of $FeL_p]^{\bullet+}$ in CH_3CN, where the reaction is, however, complete within minutes. These observations indicate that $FeL_p]^{\bullet+}$ is reduced by H_2O to the parent compound FeL_p.[74] In the reaction with water, protons are released. This leads to the masking of the $FeL_p]^{\bullet+}$ reduction reaction (eq 8) when higher concentrations of $FeL_p]^{\bullet+}$

$$FeL_p]^{\bullet+} + H_2O \rightarrow FeL_p + \text{product(s)} + H^+ \qquad (8)$$

are used. E.g., with 10 mM $FeL_p]^{\bullet+}$ in acetonitrile, the blue color of the solution does *not* change on addition of H_2O. However, on addition of 2 equiv of (solid) NaOH to the solution, the color disappears and the spectrum observed is that of FeL_p. The explanation is in terms of formation (eq 1) of $Fe_2(L_pH)_2]^{2+}$, the dimer of the parent, by the H^+ produced in the reduction reaction, eq 8. As described in section 2, the color of $Fe_2(L_pH)_2]^{2+}$ is practically the same as that of $FeL_p]^{\bullet+}$. At low amounts of H^+ produced, its concentration is not sufficient to lead to dimer formation.

The potential formation of O_2 as a product from the oxidation of H_2O was tested using gas chromatography for detection. The reactants were 10 mM $FeL_p]^{\bullet+}$ in acetonitrile and an excess of water. The limit of detection was such that a signal would have been seen if the yield of O_2 was ≥2% based on $FeL_p]^{\bullet+}$. No O_2 was seen. If the product is not O_2, it may be speculated that it should be $OH^{\bullet}$. There is only a low chance of identifying this reactive radical; if formed, it would be rapidly scavenged by the ligand or by the solvent.

That $FeL_p]^{\bullet+}$ is an oxidant can also be seen by its rapid reaction with *N,N,N′,N′*-tetramethyl-*p*-phenylenediamine (TMPD), in which the very stable and intensely colored[75] radical cation $TMPD^{\bullet+}$ is formed.

(74) A similar reaction appears to proceed in alcohols and ethers (THF, dioxane).

Summary and Conclusions

Using UV/vis, Mössbauer, and resonance Raman spectroscopies, it has been demonstrated that the species formed from $Fe^{III}L_p$ (or $Fe^{III}L_o$) by ≈250-nm photolysis in chlorinated hydrocarbons, and only in these (Φ = 0.1–0.3), or by reaction with the one-electron oxidants $SO_4^{\bullet-}$, $H_2PO_4^{\bullet}$, or $O_2^{\bullet+}$ in polar solvents such as acetonitrile is a radical cation with the unpaired spin localized on one of the phenolate moieties of the macrocyclic ligand. The oxidation state of the metal center (Fe^{III}) is *not* changed. The oxidized molecules are thus systems in which the *ligand* carries the oxidation equivalent.

It is relevant to note that our data concerning the site of electron removal (the "hole") are at variance with suggestions made for other Fe^{III} complexes containing a phenolate ligand, which were oxidized by Ce^{IV}.[76] The data were interpreted in terms of oxidation of the Fe^{III} center to yield Fe^{IV} species. However, the results, in particular the reported Mössbauer data,[76] are more readily explained in terms of high-spin Fe^{III} complexes with a coordinated ligand radical. There is the possibility that this type of behavior of phenolate-containing (macrocyclic) Fe^{III} complexes may be a general one. It is in this respect that FeL_p or FeL_o may serve as models for the active centers of certain redox-active biomolecules containing tyrosyl radicals.

Acknowledgment. We thank Professor W. Keune and Ulrich von Hörsten (Universität Duisburg) for their support in performing the Mössbauer measurements. We also thank the Deutsche Forschungsgemeinschaft (DFG) for a scholarship (J.H.) in conjunction with the project Ste 474/1-1.

(75) For the absorption spectrum, see: Fujita, S.; Steenken, S. *J. Am. Chem. Soc.* **1981**, *103*, 2540.

(76) Koikawa, M.; Okawa, H.; Maeda, Y.; Kida, S. *Inorg. Chim. Acta* **1992**, *194*, 75.